

Plastic Deformations of Unsaturated Fine-Grained Soils Under Cyclic Thermo-Mechanical Loads

C.W.W. Ng^(✉) and C. Zhou

The Hong Kong University of Science and Technology,
Kowloon, Hong Kong
cecwwng@ust.hk

Abstract. Plastic deformation of unsaturated soils under cyclic thermo-mechanical loads is important to the serviceability of many earth structures, such as the high-speed railway embankment and energy pile. In this keynote, experimental and theoretical studies of cyclic thermo-mechanical behaviour of unsaturated fine-grained soils are presented. Particular attentions are given to cyclic shear behaviour of unsaturated soil at various suctions and temperatures, as well as soil volume changes under heating and cooling at different suctions.

Introduction

Soils in many earth structures such as high-speed railway embankment and energy pile are often subjected to cyclic thermo-mechanical loads, which may induce volume changes and hence settlements. Figure 1 shows the volume change behaviour of two saturated fine-grained soils, remolded clay tested in triaxial and intact silty clay in oedometer, under cyclic heating and cooling (Campanella and Mitchell 1968; Di Donna and Laloui 2015). It is clear that with an increasing number of thermal cycles, the cumulative plastic contraction of the two soils accumulated, albeit at a decreasing rate. During the cooling phase, however, it appears that there were two opposite responses. Remolded clay expanded but intact silt contracted. No existing constitutive soil model can capture the observed cyclic behaviour of soils reported in the figure well.

In this keynote, constitutive modelling and experimental study of cyclic thermo-mechanical behaviour of two unsaturated fine-grained soils are briefly described. Particular attentions are paid to (a) plastic soil deformation induced by cyclic mechanical shearing at various suctions and temperatures; (b) soil volume changes under heating and cooling cycles. Measured results are compared with theoretical model predictions. It should be noted that some contents of this keynote are based on and extracted from Ng et al. (2016), Zhou and Ng (2016a) and Zhou and Ng (2016b).

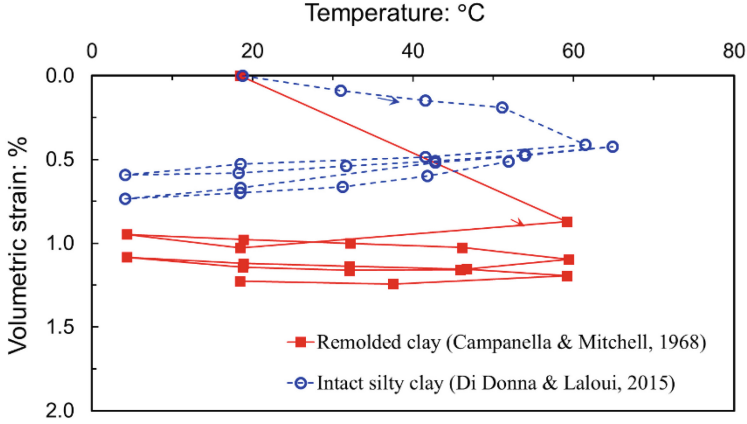


Fig. 1. Measured volume changes of saturated fine-grained soils under thermal cycles.

A Cyclic Thermo-Mechanical Model for Unsaturated Soil

Constitutive Variables

In order to analyse soil behaviour under cyclic thermo-mechanical loading at various suctions, a new constitutive soil model is formulated in the triaxial space (Zhou and Ng 2016a). Three variables are used to define the stress state of soil specimen, including mean Bishop's stress (p^*), deviator stress (q) and suction (s). Two volumetric variables, i.e., specific volume (v) and degree of saturation (S_r), are chosen to define the relative proportions of solids, water and air within an unsaturated soil element. Moreover, the temperature (T) is included to model thermal effects on soil behaviour. Apart from the above six variables, two state parameters (ξ and ψ) are adopted:

$$\xi = f(s)(1 - S_r) \quad (1)$$

$$\psi = e - e_c \quad (2)$$

where e and e_c are the current and the critical state void ratios corresponding to the current stress in the v - $\ln p^*$ plane. The state parameter ξ , which was introduced by Gallipoli et al. (2003), is used to describe the stabilisation effects on soil skeleton arising from water meniscus between soil particles approximately. According to Eq. (1), the value of ξ depends on two terms: $f(s)$ and $(1 - S_r)$. The first term $f(s)$ represents the stabilizing normal force exerted by a single water meniscus, while the second term $(1 - S_r)$ implicitly accounts for the number of water meniscus per unit soil volume. The other state parameter ψ , which was proposed by Been and Jefferies (1985), is used to describe how far the soil state is from the critical state in terms of void ratio. According to the definition in Eq. (2), positive and negative values of ψ denote soil states on the wet side and the dry side of the critical state line (CSL), respectively,

The Three Bounding Surfaces

The bounding surface plasticity theory of Dafalias (1986) is adopted in the development of the proposed model, with three bounding surfaces (F_c , F_s and F_h) constructed. The first one F_c is defined to describe elastoplastic behaviour during compression. It is well-known as loading collapse (LC) surface in the $p^*-q-\xi$ space and shown in Fig. 2. F_c can be described as:

$$F_c = p^* - p_0(T, \xi) \quad (3)$$

where $p_0(T, \xi)$ is the preconsolidation pressure,

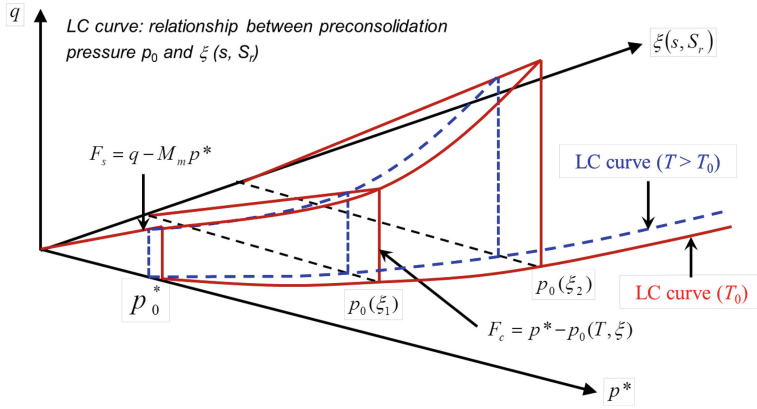


Fig. 2. Bounding surfaces F_s and F_c in the $p^* - q - \xi$ space with thermal effects.

Furthermore, $p_0(T, \xi)$ is related to normal compression lines (NCLs) and isotropic unloading-reloading lines at various conditions of T and ξ :

$$\frac{p_0(T, \xi)}{p_{atm}} = \exp \left(\frac{N(T, \xi) - v - \kappa \ln \left(\frac{p^*}{p_{atm}} \right)}{\lambda(\xi) - \kappa} \right) \quad (4)$$

where the atmospheric pressure p_{atm} (101 kPa) is included as a reference pressure; $\lambda(\xi)$ and κ are slopes of NCL and unloading and reloading line (URL) in the $v-\ln p^*$ plane, respectively; and $N(T, \xi)$ is the intercept of NCL (specific volume at the reference pressure), described by the following equation:

$$N(T, \xi) = [N_0 - r_N(T - T_0)] [1 - a(1 - \exp(b\xi))] \quad (5)$$

where N_0 is the value of $N(T, \xi)$ at zero suction and at a reference temperature; r_N , a and b are soil parameters describing suction and thermal effects on NCL. According to Eq. (5), the value of $N(T, \xi)$ decreases with an increasing temperature but with a decreasing suction. This relationship is supported by the experimental results reported

by (Zhou and Ng 2016a). Consequently, the effects of s , T and S_r on $p_0(T, \zeta)$ are included through the term $N(T, \zeta)$.

The other two surfaces F_s and F_h are relevant to elastoplastic behaviour during shearing and suction change, respectively. Details of these two boundary surfaces were reported by Zhou and Ng (2016a).

Elasto-Plasticity

For each loading process, both elastic and plastic strains can occur. Elastic and plastic strains are calculated using the following two equations:

$$\begin{cases} d\epsilon_v^e = \frac{dp^*}{K} - \frac{\alpha_{sk}}{1+e} dT \\ d\epsilon_q^e = \frac{dq}{3G_0} \\ dS_r^e = \frac{ds}{K_w} \end{cases} \quad (6)$$

$$\begin{cases} d\epsilon_v^p = \Lambda_{(c)} + D_{v(s)}\Lambda_{(s)} + D_{v(h)}\Lambda_{(h)} \\ d\epsilon_q^p = D_{q(c)}\Lambda_{(c)} + \Lambda_{(s)} + D_{q(h)}\Lambda_{(h)} \\ dS_r^p = D_{w(c)}\Lambda_{(c)} + D_{w(s)}\Lambda_{(s)} + \Lambda_{(h)} \end{cases} \quad (7)$$

where $d\epsilon_v^e$ and $d\epsilon_v^p$ are the elastic and plastic volumetric strains respectively; $d\epsilon_q^e$ and $d\epsilon_q^p$ are the elastic and plastic shear strains respectively; dS_r^e and dS_r^p are the elastic and plastic increments of S_r respectively; K is the elastic bulk modulus for soil skeleton; G_0 is the very small strain shear modulus; K_w is the ratio of incremental suction to elastic decrement of degree of saturation; and α_{sk} is isotropic thermal expansion coefficients for soil skeleton; $\Lambda_{(c)}$, $\Lambda_{(s)}$ and $\Lambda_{(h)}$ are the loading indices for compression, shearing and suction change mechanism respectively; $D_{q(c)}$, $D_{w(c)}$, $D_{v(s)}$, $D_{w(s)}$, $D_{v(h)}$ and $D_{q(h)}$ are the dilatancy factors. Experimental results in the literature generally seem to suggest that soil response upon cooling may be idealized as elastic and reversible (Hong et al. 2013). For simplicity, the same assumption is adopted in this current study. More discussion is given in the section of “Interpretations of measured and computed results”.

Equation (7) does not explicitly consider thermally induced plastic increments of strain and degree of saturation. Any phenomenon of thermo-plasticity is implicitly taken into account. This is because normal compression line, critical state line in the v - $\ln p^*$ plane and water retention curve in the current model are all temperature-dependent. A change of temperature would alter the location of bounding surfaces for the plastic mechanism of shearing, compression and suction change. The loading indices $\Lambda_{(c)}$, $\Lambda_{(s)}$ and $\Lambda_{(h)}$ in Eq. (7) are therefore all dependent on temperature, determined through hardening law and condition of consistency. From the bounding surface F_s , $\Lambda_{(s)}$ is calculated using the following equations:

$$A_{(s)} = \frac{1}{K_s^p} (dq - M_m dp^*) \quad (8)$$

$$K_s^p = \frac{G_0 h}{M_m} \left(M \exp(-n_b \psi) \left(\frac{\bar{\rho}_s}{\rho_s} \right) - M_m \right) \quad (9)$$

where h and n_b are soil parameters; ρ_s and $\bar{\rho}_s$ are Euclidian distances with respective to shearing, depending on the last loading reversal, current and maximum stress ratios. The value of $\rho_s/\bar{\rho}_s$ is zero when there is a 180° reversal in the stress path and approaches 1 as soil stress state moves towards F_s . It can be deduced from Eq. (9) that plastic modulus K_s^p decrease as the ratio $\rho_s/\bar{\rho}_s$ increases. This is consistent with experimental observation that larger plastic strain would be induced as stress state approaches bounding surface. This is one of the key features of the proposed model different from other conventional elastoplastic models for unsaturated soils (e.g., Alonso et al. (1990) and Chiu and Ng (2003)). In these previous models, soil response is assumed to be purely elastic when soil state is inside bounding (yield) surface. In addition, $A_{(c)}$ and $A_{(h)}$ in Eq. (7) can be determined based on the condition of consistency for bounding surfaces F_c and F_h , respectively. More details of the proposed cyclic thermo-mechanical model is given by Zhou and Ng (2016a).

Test Apparatuses

To test unsaturated soil at various temperatures, a suction-controlled triaxial apparatus was developed to allow for independent control of suction and temperature. To apply thermal loads, a heating system was installed. The system adopted the axis-translation technique to control matric suction. In order to avoid possible compliance errors by using externally mounted LVDT, internal Hall-effect transducers were adopted to measure local strains at centre portion of each soil specimen. The accuracy is about $3 \mu\text{m}$, corresponding to vertical strains of about 0.003%. Careful calibration tests show that the suction probe and Hall effect transducer are both sufficiently temperature compensated in the temperature range from 20 to 60 °C. Details of the cyclic triaxial system and measuring devices were reported by Ng and Zhou (2014).

To investigate soil behaviour under heating and cooling cycles, a double cell triaxial system (Ng and Menzies 2007) was modified by installing a temperature control system. Figure 3 shows a schematic diagram of the modified double cell triaxial system. Compared to the cyclic triaxial system above, the double cell triaxial system is able to apply not only heating but also for cooling soil specimen incrementally. Furthermore, a much smaller specimen height of 20 mm can be used in this apparatus to reduce suction equalisation time. Soil temperature can reach the target temperature within six hours. Similar to the cyclic triaxial system, the axis translation technique is used to control the matric suction of soil specimen. After calibration, the accuracy of volumetric strain measurement is 0.03%. Details of the temperature-controlled double cell system and calibration methods were reported by Ng et al. (2016).

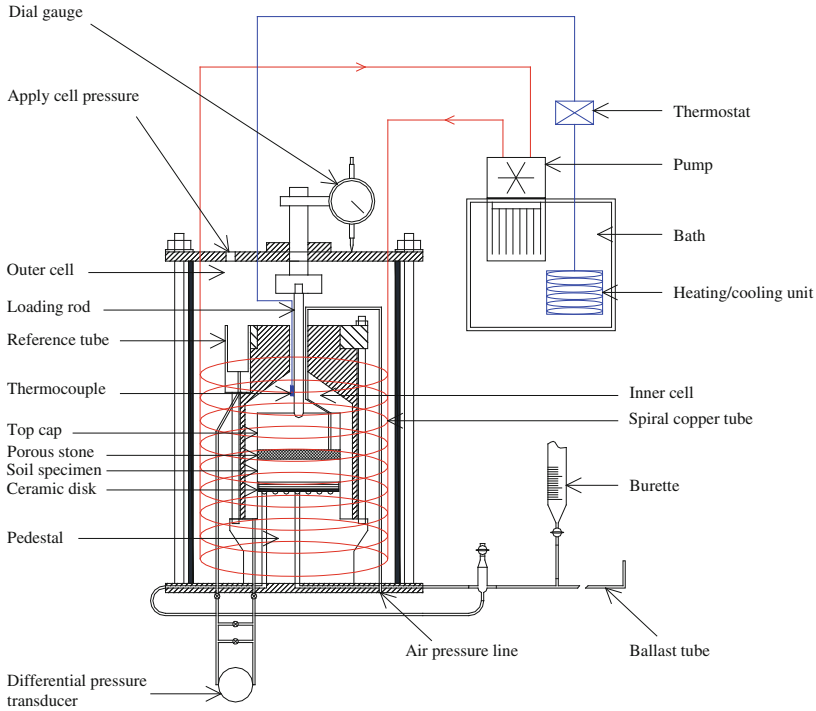


Fig. 3. Schematic diagram of suction- and temperature-controlled double cell triaxial system (Ng et al. 2016).

Test Soils and Specimen Preparation

Two fine-grained soils tested are reported in this study: recompacted silt and intact and recompacted clay. The silt tested is a yellowish-brown completely decomposed coarse ash tuff (CDT), commonly found in Hong Kong and often used as construction material. Following the Unified Soil Classification System (ASTM 2011), CDT is classified as silt (ML). Each triaxial specimen, 76 mm in diameter and 152 mm in height, was compacted in 10 layers at optimum water content of about 16.3% and dry density of about 1760 kg/m^3 . The initial suction after compaction is $95 \pm 2 \text{ kPa}$ as measured by a high capacity suction probe.

The clay tested is a loess soil taken from Shaanxi Province, China. It is an aeolian sediment. According to the Unified Soil Classification System (ASTM 2011), the loess is classified as a clay of low plasticity (CL). Following the sampling procedures specified by GEO (2000), intact block loess samples were manually extracted. In the laboratory, a cutter ring with 76 mm diameter and 20 mm height was used to obtain the intact specimens. The initial void ratio was about 1.17 and the initial suction was $200 \pm 20 \text{ kPa}$. For recompacted specimens, static compaction was adopted. Each specimen, 76 mm in diameter and 20 mm in height, was statically compacted in 2 layers. The compaction water content and void ratio were 10.9% and 1.17, respectively.

These properties were controlled to be the same as the initial state of the intact specimens for later comparison.

Test Program and Procedures

Series A: Mechanical Cyclic Shear Tests on CDT at Various Suctions and Temperatures

To investigate thermal effects on mechanical cyclic behaviour of unsaturated CDT, nine triaxial tests were carried out at three temperatures (i.e., 20, 40 and 60 °C). Three levels of soil suction (i.e., 0, 30 and 60 kPa) were considered and used at each temperature. There were four stages in each temperature- and suction-controlled cyclic triaxial test, including isotropic consolidation, suction equalisation, thermal equalisation and cyclic loading-unloading. Figure 4 shows the thermo-hydro-mechanical path of each test in the first three stages. These three stages are designed to control soil specimen to the target stress, suction and temperature, respectively. At the last stage of each test, soil specimen was subjected to cyclic shearing. Cyclic deviator stress in the haversine form was applied while net confining pressure was maintained at 30 kPa. The difference between maximum and minimum applied deviator stresses is defined as cyclic deviator stress q_{cyc} . Four levels of cyclic stress (30, 40, 55 and 70 kPa) were applied to each specimen in succession. At each level of q_{cyc} , 100 cycles were applied at a frequency of 1 Hz. More details of this series of tests were given by Ng and Zhou (2014).

Series B: Heating and Cooling Cyclic Tests on Loess

Four heating and cooling cyclic tests were carried out at different suctions and temperatures. Two of them (R0 and R100) were carried out on recompacted loess specimens but at different suctions (0 and 100 kPa). The other two (I0 and I100) were carried out on intact loess specimens at suctions of 0 and 100 kPa. Figure 5 shows the

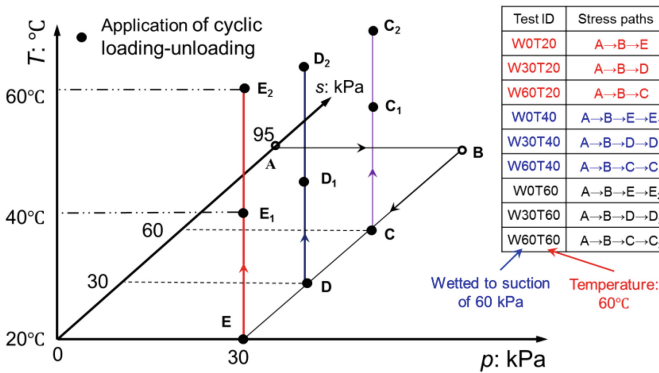


Fig. 4. Stress path of suction and temperature controlled cyclic shear tests (Series A).

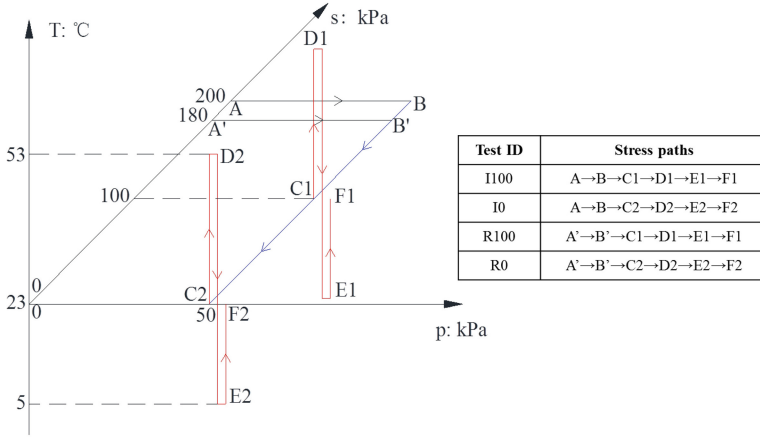


Fig. 5. Stress path of cyclic heating and cooling tests (Series B).

thermo-mechanical loading paths of the loess specimens. Each test consisted of three stages: isotropic compression, wetting and thermal cycle. More details of this series of tests were given by Ng et al. (2016).

Comparisons of Measured and Computed Results

Cyclic Stress-Strain Relations at Various Suctions and Temperatures

Figure 6 compares the measured and computed cyclic stress-strain relations of recompact CDT specimens at zero suction but at different temperatures (20 and 60 °C) (refer to tests WOT20 and WOT60 in Fig. 4). At each temperature, there was an increase in the measured accumulation of plastic strain with the number of cycles. It is evident that the measured behaviour such as the non-linearity and hysteresis of stress-strain relations during unloading and reloading cycles can be captured by the new constitutive model presented in previous section reasonably well. This is mainly because the proposed model incorporates effects of stress reversal and strain on soil behaviour. When the loading direction changes (180° reversal in the stress path), the value of $\rho_s/\bar{\rho}_s$ becomes zero and therefore the value of Kp_s becomes very large (see Eq. (9)). Soil response is essentially elastic at the beginning of each loading or unloading process. During subsequent shearing with an increasing strain, the value of $\rho_s/\bar{\rho}_s$ continues to increase. Hence, the plastic modulus becomes smaller and larger plastic strain would be predicted.

As shown in the figure, the cyclic stress-strain relations follow the same trend at zero suction but at different temperatures. Furthermore, the measured accumulation of plastic strains increased with an increase in temperature. The observed thermal effects on the accumulated plastic strains can be theoretically explained by thermal softening. According to Eqs. (3), (4) and (5), the preconsolidation pressure $p_0(T, \xi)$ is smaller at a higher temperature. With a smaller preconsolidation pressure and hence a lower OCR, soil specimen behaves softer.

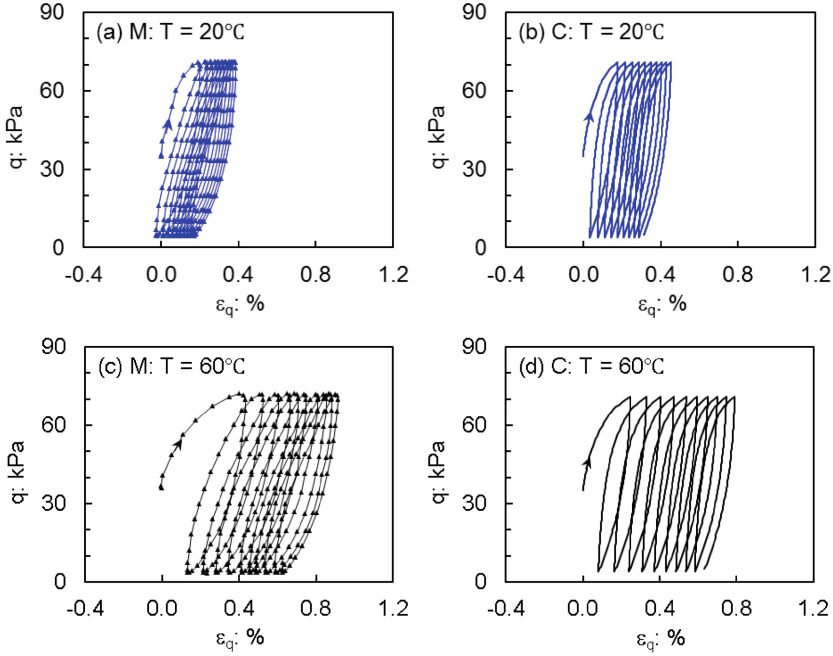


Fig. 6. Measured (M) and computed (C) cyclic stress-strain relations at different temperatures and at zero suction of CDT.

Effects of Number of Mechanical Load Cycles on Plastic Strain Accumulation at Various Suctions and Temperatures

Figure 7 shows the influence of suction and temperature on the relationship between $\varepsilon_{ap(100)}/\varepsilon_{ap(1)}$ and q_{cyc} , where $\varepsilon_{ap(1)}$ and $\varepsilon_{ap(100)}$ are plastic strains induced by the first cycle and 100 cycles, respectively. At three different suctions (0, 30 and 60 kPa) and at 20 °C (i.e., tests W0T20, W30T20 and W60T20), all three measured relationships between $\varepsilon_{ap(100)}/\varepsilon_{ap(1)}$ and q_{cyc} were similar, when applied q_{cyc} was between 30 and 40 kPa. When q_{cyc} was increased from 40 kPa to 70 kPa, however, the ratio of $\varepsilon_{ap(100)}/\varepsilon_{ap(1)}$ increased significantly by about 40% at zero suction. On the contrary, the ratios of $\varepsilon_{ap(100)}/\varepsilon_{ap(1)}$ appeared to be independent of q_{cyc} at suctions of 30 and 60 kPa. These observations can be explained by the existence of threshold q_{cyc} values at various suctions. As observed by Zhou and Ng (2016b), the threshold q_{cyc} at zero suction is below 70 kPa. With a significant increase in preconsolidation pressure with increasing suction (illustrated by the LC curve in Fig. 2 conceptually), the threshold q_{cyc} is larger than 70 kPa at suctions of 30 and 60 kPa (Zhou and Ng 2016b). Consequently, at q_{cyc} of 30 and 40 kPa, which are lower than threshold q_{cyc} at all $u_a - u_w$, the ratio $\varepsilon_{ap(100)}/\varepsilon_{ap(1)}$ is almost independent of $u_a - u_w$. At q_{cyc} of 70 kPa, which is higher than the threshold stress at zero suction but lower than the threshold stress at $u_a - u_w$ of 30 and 60 kPa, $\varepsilon_{ap(100)}/\varepsilon_{ap(1)}$ decreases with an increase in $u_a - u_w$. The existence of a threshold q_{cyc} should be considered in the geotechnical designs. To minimize plastic

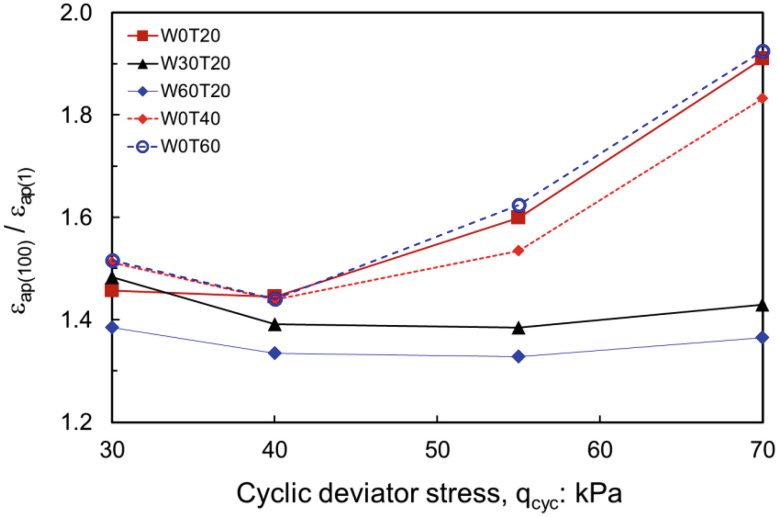


Fig. 7. Influence of number of cycles on plastic strain accumulation at different suctions and temperatures of CDT.

strain accumulation of soils and to improve long-term performance of earth structures, the design cyclic loads should be kept lower than the threshold value.

It can be also seen from Fig. 7 the measured ratio of $\epsilon_{ap(100)}/\epsilon_{ap(1)}$ decreased slightly from when q_{cyc} was increased from 30 to 40 kPa, at zero suction and at three different temperatures (i.e., tests W0T20, W0T40 and W0T60). Beyond 40 kPa, the ratio increased with an increase in q_{cyc} . It is evident that the relationship between $\epsilon_{ap(100)}/\epsilon_{ap(1)}$ and q_{cyc} is almost independent of temperature. Temperature-induced differences in $\epsilon_{ap(100)}/\epsilon_{ap(1)}$ are all less than 10% at the three temperatures. The negligible difference in $\epsilon_{ap(100)}/\epsilon_{ap(1)}$ at various temperatures is likely because in the temperature range of 20 to 60 °C, thermal effects on the threshold q_{cyc} is very minor (Zhou and Ng 2016b).

Influence of Temperature on Plastic Strain Accumulation

Figure 8 shows the effects of temperature on $\epsilon_{ap(100)}$ at two different suctions (0, and 60 kPa) of CDT. It is clear that the influence of temperature on $\epsilon_{ap(100)}$ are qualitatively similar at different suctions. At a given suction, $\epsilon_{ap(100)}$ increases consistently with an increase in temperature at q_{cyc} of 30, 40, 55 and 70 kPa. The measured $\epsilon_{ap(100)}$ at 60 °C is about two times of that at 20 °C. For the recompacted CDT specimens, the pre-consolidation pressure is beyond 100 kPa, which is much larger than the net confining stress of 30 kPa. It is therefore that soil stress state was inside bounding surface during the heating process. According to the thermo-mechanical model illustrated in Fig. 2,

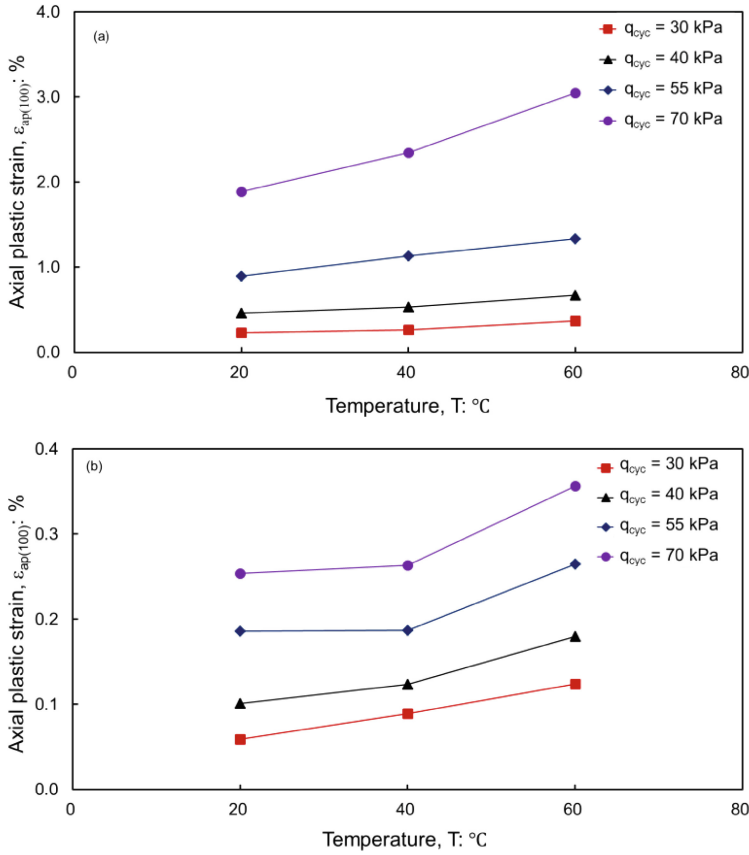


Fig. 8. Thermal effects on plastic strain accumulation of CDT at (a) $s = 0$ kPa and (b) $s = 60$ kPa.

the preconsolidation pressure should decrease with an increase in temperature. For example, as temperature increases from 20 to 40 °C, the OCR decreases by about 10% and the axial plastic strain increases by about 30%. Given a smaller overconsolidation ratio, it is expected that a larger axial plastic strain should be induced in the heated specimen during the subsequent stage of cyclic loading-unloading.

As far as the authors are aware, the current geotechnical design guides (for instance, design methods for railway embankments and pavements) generally do not consider thermal effects on soil behaviour since soil specimen is only required to be tested at room temperature (AASHTO 2008). When the in-situ temperature is significantly higher than room temperature, ignoring thermal effects may underestimate the irreversible ground settlement induced by cyclic loads significantly.

Influence of Suction on Plastic Strain Accumulation of CDT

It is clearly revealed in Fig. 8 that at a given temperature and q_{cyc} , $\varepsilon_{ap(100)}$ decreases significantly with increasing suction. For example, at q_{cyc} of 70 kPa and 20 °C, $\varepsilon_{ap(100)}$ decreases from about 2% to 0.25% as $u_a - u_w$ increases from 0 to 60 kPa. The percentage of reduction is up to about 90%. The decrease in $\varepsilon_{ap(100)}$ with an increase in suction is mainly because as suction increases, the preconsolidation pressure of soil specimen increases, as illustrated in Fig. 2. Given a larger preconsolidation pressure and hence a higher OCR, soil specimen behaves stiffer, as described by Eq. (9).

Some current geotechnical design guides have considered effects of soil moisture on soil behaviour using empirical methods. For example, AASHTO (2008) for pavement design suggests that soil specimen is prepared and tested at a reference moisture condition. Variations in soil behaviour with soil moisture are then estimated using some empirical models. Since the relationship between axial plastic strain and suction depends on temperature, as illustrated in Fig. 8, regression parameters in these empirical models should be a function of temperature.

Volume Change Behaviour of Loess During Thermal Cycles

Figure 9 shows the observed volumetric behaviour of recompacted and intact loess specimens during heating and cooling cycles at two different suctions, i.e., 0 and 100 kPa, obtained from tests in Series B. During the heating process, the measured contractive volumetric strain increased with increasing temperature and at an increasing rate. The observed heating-induced soil contraction can be explained using the proposed bounding surface model. According to Eqs. (3) through (5), the pre-consolidation pressure decreases as temperature increases. During the heating process, soil state approaches F_c surface, resulting in plastic contraction.

When temperature decreases from 53 to 13 °C, the measured contractive volumetric strain of intact and recompacted specimens increased, but at a much slower rate of around $2 \times 10^{-3}\%/^{\circ}\text{C}$ (close to thermal expansion coefficient of clay (about $2.9 \times 10^{-3}\%/^{\circ}\text{C}$)). This process may be considered as that the soil state is within the bounding surface, meaning that it is an essentially elastic deformation due to thermal contraction of soil particles. When temperature keeps decreasing, from 13 to 5 °C, a plastic contractive volumetric strain at a larger rate of $2.5 \times 10^{-2}\%/^{\circ}\text{C}$ can be observed, suggesting that plastic strain is induced by cooling to 5 °C, which is close to the critical temperature (i.e., 4 °C) of water at which water should have the largest density. This may imply that a volume reduction of water would be expected for a given mass of water, leading to an extra plastic deformation of water and re-arrangement of soil structure.

It should be pointed out that cooling-induced plastic strain is different from previous studies on saturated soils. As discussed in the introduction, Campanella and Mitchell (1968) and Di Donna and Laloui (2015) measured volume changes of saturated remolded illite and natural silty clay during cooling from 60 to 5 °C. For both soils, only elastic contraction and slight expansion were observed during cooling. The discrepancy between the current study and the two previous studies may be because the

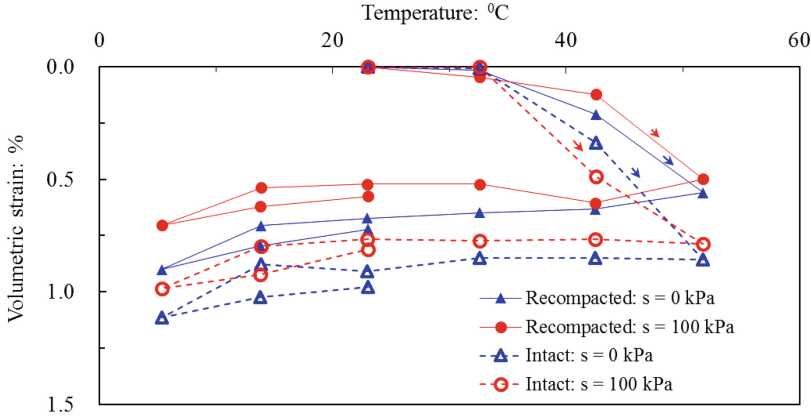


Fig. 9. Measured volume changes of intact and recompacted loess under thermal loads.

void ratio of loess specimen (at both intact and recompacted states) is about 20% and 60% larger than those of the remolded illite and natural silty clay specimens, respectively. Given a much larger void ratio, some large voids of loess are unstable (Sun et al. 2007) and can be destroyed by cooling-induced particle contraction. Consequently, cooling may induce particle re-arrangement and plastic contraction in the loess specimen.

The observed plastic contraction of intact and recompacted specimens during cooling from 15 °C to 5 °C cannot be predicted by any existing elasto-plastic theory, which generally predicts elastic contraction during cooling. A new ‘temperature decrease, TD’ bounding surface may be introduced in existing elastoplastic thermo-mechanical models to simulate the observed elasto-plastic behaviour during cooling, as shown in Fig. 10. When temperature is high than the critical value (1 → 2)

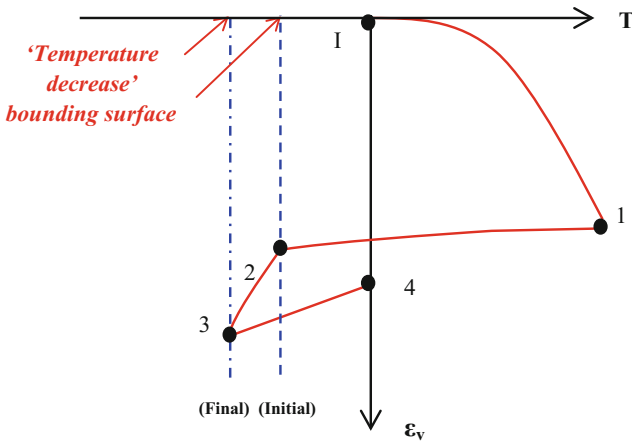


Fig. 10. Proposed temperature decrease (TD) bounding surface.

corresponding to the TD bounding surface, soil response may be assumed to be elastic. When soil state reaches the TD bounding surface, soil response under continuous cooling is regarded as elastoplastic ($2 \rightarrow 3$).

Summary and Conclusions

Based on measured and computed results, key conclusions are summarized as follows:

(1) During cyclic mechanical shearing, measured plastic deformation of completely decomposed silt (CDT) increases continuously with an increase in q_{cyc} at a given suction and temperature. The rate of increase is almost constant at q_{cyc} lower than a threshold value, but increases significantly at q_{cyc} higher than the threshold value. The existence of a threshold q_{cyc} implies that the applied cyclic loads should be lower than this threshold value in order to minimize plastic strain accumulation of soils and to improve long-term performance of earth structures.

(2) Measured plastic deformation of unsaturated CDT increases significantly with decreasing suction and increasing temperature. The observed effects of suction and temperature can be explained by the fact that preconsolidation pressure of the unsaturated soil increases with increasing suction (suction hardening), but decreases with increasing temperature (thermal softening). Since the current geotechnical designs of railway embankments and subgrade soils of pavement generally use soil parameters determined at room temperature only, soil deformation induced by cyclic mechanical loads may be significantly underestimated.

(3) As temperature increases from 23 to 53 °C incrementally, contractive volumetric strain of both intact and recompacted loess specimens increases. During the cooling process from 53 to 13 °C, contractive volumetric strain (essentially elastic) keeps increasing at a much reduced rate. When temperature further decreases from 13 to 5 °C, a plastic volume contraction at a much higher rate is observed. To simulate the observed plastic response during cooling, a new 'temperature decrease, TD' bounding surface may be introduced in existing models.

Acknowledgements. The authors would like to acknowledge the contributions from research grant 51509041 provided by the National Science Foundation of China and also the grants 16209415, 16216116, 617213 and HKUST6/CRF/12R supported by the Research Grants Council (RGC) of the HKSAR.

References

- AASHTO (2008) Mechanical empirical pavement design guide: a manual of practice. American Association of State Highway and State Highway Officials, Washington, DC
- Alonso EE, Gens A, Josa A (1990) Constitutive model for partially saturated soils. *Géotechnique* 40(3):405–430
- ASTM (2011) Standard practice for classification of soils for engineering purposes (unified soil classification system). American Society of Testing and Materials, West Conshohocken
- Been K, Jeffries MG (1985) A state parameter for sands. *Géotechnique* 35(2):99–112

- Campanella RG, Mitchell JK (1968) Influence of temperature variations on soil behavior. *J Soil Mech Found Div* 94(3):709–734
- Chiu CF, Ng CWW (2003) A state-dependent elasto-plastic model for saturated and unsaturated soils. *Géotechnique* 53(9):809–830
- Dafalias YF (1986) Bounding surface plasticity. I: mathematical foundation and hypoplasticity. *J Eng Mech* 112(9):966–987
- Di Donna A, Laloui L (2015) Response of soil subjected to thermal cyclic loading: experimental and constitutive study. *Eng Geol* 190:65–76
- Gallipoli D, Gens A, Sharma R, Vaunat J (2003) An elasto-plastic model for unsaturated soil incorporating the effects of suction and degree of saturation on mechanical behaviour. *Géotechnique* 53(1):123–135
- GEO (2000) *Geoguide 2: guide to site investigation*. Geotechnical Engineering Office of Hong Kong government
- Hong PY, Pereira JM, Tang AM, Cui YJ (2013) On some advanced thermo-mechanical models for saturated clays. *Int J Numer Anal Meth Geomech* 37(17):2952–2971
- Ng CWW, Cheng Q, Zhou C, Alonso EE (2016) Volume changes of an unsaturated clay during heating and cooling. *Géotechnique Lett* 6(3):192–198
- Ng CWW, Menzies B (2007) *Advanced unsaturated soil mechanics and engineering*. Taylor & Francis, London
- Ng CWW, Zhou C (2014) Cyclic behaviour of an unsaturated silt at various suctions and temperatures. *Géotechnique* 64(9):709–720
- Sun DA, Sheng DC, Xu Y (2007) Collapse behaviour of unsaturated compacted soil with different initial densities. *Can Geotechnical J* 44(6):673–686
- Zhou C, Ng CWW (2016a) Simulating the cyclic behaviour of unsaturated soil at various temperatures using a bounding surface model. *Géotechnique* 66(4):344–350
- Zhou C, Ng CWW (2016b) Effects of temperature and suction on plastic deformation of unsaturated silt under cyclic loads. *J Mater Civil Eng* 28(12):04016170. ASCE

Advances in Laboratory Testing and Modelling of Soils
and Shales (ATMSS)

Ferrari, A.; Laloui, L. (Eds.)

2017, XII, 527 p. 337 illus., 223 illus. in color.,

Hardcover

ISBN: 978-3-319-52772-7